

We are IntechOpen, the world's leading publisher of Open Access books Built by scientists, for scientists

6,900

Open access books available

185,000

International authors and editors

200M

Downloads

Our authors are among the

154

Countries delivered to

TOP 1%

most cited scientists

12.2%

Contributors from top 500 universities



WEB OF SCIENCE™

Selection of our books indexed in the Book Citation Index
in Web of Science™ Core Collection (BKCI)

Interested in publishing with us?
Contact book.department@intechopen.com

Numbers displayed above are based on latest data collected.
For more information visit www.intechopen.com



Modeling and Simulation of Offshore Wind Farms for Smart Cities

*Cheng Siong Chin, Chu Ming Peh
and Mohan Venkateshkumar*

Abstract

Wind turbine models and simulations are widely available, but the simulation of a wind farm is scarce. This chapter presents a systematic approach to simulate an offshore wind farm for smart cities. The subsystems of several variable-pitch wind turbines, namely, rotor blades, drivetrain, and induction generator, are modeled to form a wind farm. The total output power of the wind farm by considering multiple wind turbines with the wake losses (using the Jensen wake model) can be simulated with any input wind speed. In order to validate the accuracy of the simulation, a case study was performed on a German offshore wind farm called NordseeOst. The simulation shows promising results with an average error of approximately 5% when compared with the real-time output of the wind farm. The results showed that the simulation of a wind farm that often impeded by the lack of exact information is feasible before any site implementation for smart cities.

Keywords: variable-pitch wind turbine, modeling and simulation, offshore wind farm, smart cities

1. Introduction

As a measure to resolve the declining rate of fossil fuels and the current state of emission levels, renewable energy has become an attractive source of clean and sustainable energy. The wind is a powerful and abundant source of renewable energy. Wind power installations, both onshore and offshore, have expanded rapidly over the world to harness the energy from wind. However, these wind power plants are not cheap for offshore installations. Hence, the inception of a wind farm entails many considerations and careful planning to justify the associated high cost. As a result, alternative consideration is the wind farm layout that can be optimized to increase the profitability [1].

However, the optimization of the layout is a complicated and challenging process due to a phenomenon known as wake effect. After a turbine extracts wind energy [2], the downstream wind will be turbulent and reduced in speed. It is essential to consider the wake losses when positioning the turbines to maximize energy production taking into account the additional costs for infrastructure if they are spaced far apart. By using modeling and simulation as a tool, analysis can assist

in managerial and technical decisions [3]. It is to be mentioned that manufacturer-specific models are sometimes not easy to obtain [4].

Presently, there are few studies performed on wind turbine modeling. Some examples of these studies are available [5–7]. The focus of their works was primarily on the wind turbine dynamics and its efficiency. They did not consider the implementation of a wind farm or multiple wind turbines. Nevertheless, there are a few researches conducted on wind farm simulation. For instance, the wake loss was not taken [8] into account. Hence, there is a need to systematically model the wind farm instead of just a wind turbine with the wake losses. The wind farm simulation tool should be widely available to users to simulate the feasibility of the wind turbines on the specific site before actual implementation. The approach adopted in this study encompasses the different wind speed for each turbine with consideration of wake losses. The main contribution is to provide a systematic approach to model the output power from the wind farm by considering the wake losses before implementing the wind turbines on the actual site for smart cities.

The chapter is organized as follows. In Section 2, a proposed modeling methodology is presented followed by Section 3 on a simulation model of NordseeOst wind farm. Section 4 describes the results and discussion followed by the conclusion in Section 5.

2. Modeling methodology

The NordseeOst, an operational offshore wind farm in Germany, will be used here as a case study, and the wind turbines are modeled based on the governing equations that can be implemented through the function block available in the Simulink Library. The parameters for the wind turbine model will be based on manufacturer Senvion 6.2M126 used in the German farm. The turbine model is duplicated and positioned to follow the layout of NordseeOst wind farm. By considering the wake losses of each turbine using the Jensen wake model, the wind speed input for the turbines can be computed. The wind conditions and temperature in the wind farm site will be obtained from an online resource. For any given timeframe, the output power of the simulated farm can be determined and verified with the real-time data obtained from the actual farm.

2.1 Wind turbine modeling

Multiple wind turbine models were created to form the wind farm. From a modeling viewpoint, the turbine model can be broken down into three blocks, aerodynamic, mechanical, and electrical, as shown in **Figure 1**. When the passing wind interacts with the rotor blades, lift and drag forces create the rotation of the turbine blades. This turning force is high in torque, but the speed is low. The speed of the rotating rotor shaft will be increased using a gearbox. The purpose of increasing the rotational speed is to match the requirements of the generator. The turbine and generator shaft is coupled as a drivetrain to transmit the driving force to the generator. The electrical block consists of the generator that creates a magnetic field from the rotor into electrical energy. Each block is modeled using few differential and algebraic equations that describe their functions.

2.1.1 Aerodynamic block

The aerodynamic block is characterized by three subsystems, namely, the tip speed ratio, power coefficient, and rotor torque, that are developed. The maximum

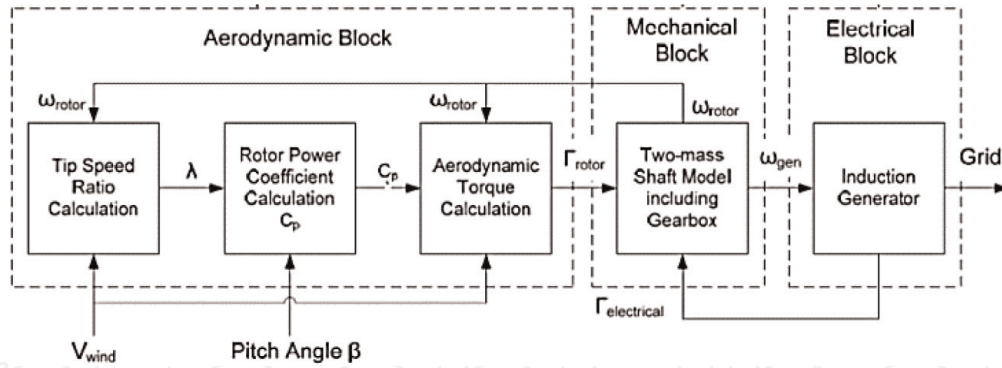


Figure 1.
 Wind turbine model [4].

power that can be extracted from the wind is 59.26% [9]. The power coefficient C_P expresses the ratio of extractable power by the rotor to the available power in the wind. The amount of power that can be extracted is given as follows:

$$P_r = \frac{1}{2} \cdot \rho \cdot A \cdot v^3 \cdot C_P(\lambda, \beta) \quad (1)$$

where ρ is the density of air in kg/m^3 , A is the rotor swept area in m^2 , v is the wind speed in m/s , and C_P is the power coefficient.

The density of air can be determined from the turbine elevation above sea level [3]:

$$\rho = \rho_o - 1.194 \times 10^{-4} \cdot H \quad (2)$$

where ρ_o is the density of air at the sea level at a specific temperature in kg/m^3 and H is the hub height in m .

The efficiency of the rotor can be described by power coefficient C_P since it is a ratio of extracted power to available wind power. It is usually expressed as a function of tip speed ratio and blade pitch angle. The ratio of linear speed at the rotor blade tip to the wind speed is defined as tip speed ratio λ as shown:

$$\lambda = \frac{\omega_r \cdot r}{v} \quad (3)$$

where ω_r is the rotor angular velocity in rad/s , r is the radius of the rotor (blade length + hub radius) in m , and v is the wind speed in m/s .

For a specific airfoil type, the power coefficient may be expressed as a function of the tip speed ratio and blade pitch angle as follows [8]:

$$C_P(\lambda, \beta) = c_1(c_2/\lambda_i - c_3\beta - c_4)e^{-c_5/\lambda_i} + c_6\lambda \quad (4)$$

where $c_1 = 0.5176$, $c_2 = 116$, $c_3 = 0.4$, $c_4 = 5$, $c_5 = 21$, and $c_6 = 0.0068$ with λ_i defined as

$$\frac{1}{\lambda_i} = \frac{1}{\lambda + 0.08\beta} - \frac{0.035}{\beta^3 + 1} \quad (5)$$

where λ is the tip speed ratio and β is the blade pitch angle.

The rotor torque developed by the turbine can be calculated as follows:

$$\Gamma_r = \frac{P_r}{\omega_r} \quad (6)$$

where Γ_r is the torque developed at the rotor in Nm, P_r is the power developed by the rotor in W, and ω_r is the rotor angular speed in rad/s.

2.1.2 Mechanical block

The purpose of a drivetrain is to transmit the torque generated by the rotor blades from the rotor hub to the generator. The torque generated is filtered by the drivetrain via the gearbox and ultimately drives the generator shaft. In this mechanical block, the drivetrain is modeled by a two-lumped-mass model as shown in **Figure 2**. The two-mass model [10] is accurate enough for the analysis of transient stability in wind power generation systems when compared with higher-order drivetrain model with three or six masses:

The stiffness and damping of the low-speed shaft are represented by a spring and damper with coefficient k_{ls} and c_{ls} , respectively. The equation of motion for the turbine rotor is expressed as follows:

$$\dot{\Omega}_r(t) = \frac{T_a(t) - T_{ls}(t) - c_f \Omega_r(t)}{J_r} \quad (7)$$

where Ω_r is the rotor angular speed in rad/s, T_a is the aerodynamic torque developed by rotor in Nm, T_{ls} is the torque of the low-speed shaft in Nm, c_f is the frictional damping, and J_r is the inertia of rotor in kgm^2 .

The mechanical torque of the shaft is modeled as follows:

$$T_{ls}(t) = k_{ls}[\theta_r(t) - \theta_{ls}(t)] + c_{ls}[\Omega_r(t) - \Omega_{ls}(t)] \quad (8)$$

where T_{ls} is the torque of low-speed shaft in Nm, k_{ls} is the stiffness coefficient, θ_r is the rotor angular position in rad, θ_{ls} is the angle of low-speed shaft in rad, c_{ls} is the damping coefficient, Ω_r is the rotor angular speed in rad/s, and Ω_{ls} is the angular speed of low-speed shaft in rad/s.

Assuming an ideal gearbox, the step-up ratio of the transmission speed is shown:

$$\eta_g = \frac{T_{ls}(t)}{T_{hs}(t)} = \frac{\Omega_g(t)}{\Omega_{ls}(t)} = \frac{\theta_g(t)}{\theta_{ls}(t)} \quad (9)$$

where T_{ls} is the torque of the low-speed shaft in Nm, T_{hs} is the torque provided to the generator in Nm, Ω_g is the angular speed of generator shaft in rad/s, Ω_{ls} is the angular speed of the low-speed shaft in rad/s, θ_g is the angle of generator shaft in rad, and θ_{ls} is the angle of the low-speed shaft in rad.

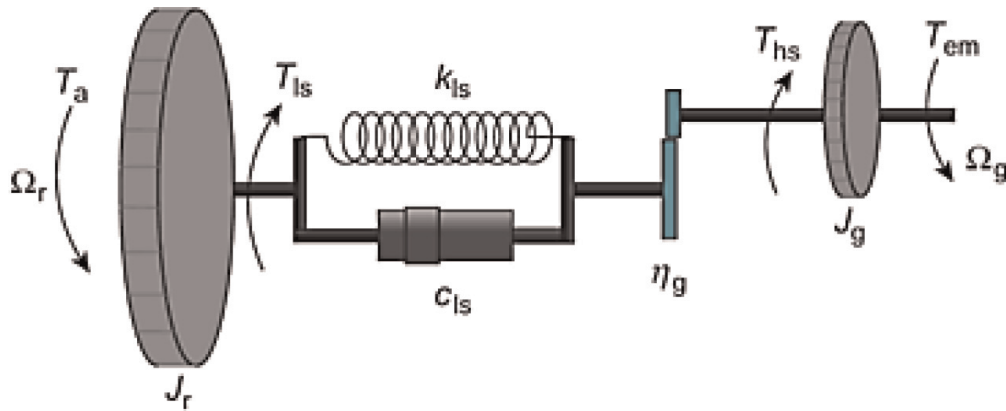


Figure 2.
Two-mass model [10].

The equation of motion for the shaft at induction generator is written as shown:

$$\dot{\Omega}_g(t) = \frac{T_{hs}(t) - T_{em}(t) - c_g \Omega_g(t)}{J_g} \quad (10)$$

where T_{hs} is the torque provided to the generator in Nm, T_{em} is the electromagnetic torque in Nm, c_g is the damping experienced at the generator, Ω_g is the angular speed of generator shaft in rad/s, and J_g is the inertia generator in kgm^2 .

2.1.3 Electrical block

The ideal induction generator dynamic model consists of three stators and three winding rotors. The differential equations are derived from the state space vector representation using synchronous reference frame for the d-q model. The modeling is simplified and preferable when represented as DC values. In order to do so, the stator and rotor are each transferred onto a direct and quadrature axis (d-q model). The direct and quadrature axes for the stator are represented by ds and qs , respectively. The same axis for the rotor can also be represented by dr and qr . To simulate the induction generator, an equation to represent both the direct and quadrature axis voltages for the stator V_{ds} , V_{qs} and current I_{ds} , I_{qs} is required. Eqs. (11)–(18) are the models of an induction generator expressed in a d-q reference frame [3].

The stator and rotor magnetic flux linkages are given as follows:

$$\varphi_{ds} = X_s \cdot I_{ds} + X_m \cdot I_{dr} \quad (11)$$

$$\varphi_{qs} = X_s \cdot I_{qs} + X_m \cdot I_{qr} \quad (12)$$

$$\varphi_{dr} = X_r \cdot I_{dr} + X_m \cdot I_{ds} \quad (13)$$

$$\varphi_{qr} = X_r \cdot I_{qr} + X_m \cdot I_{qs} \quad (14)$$

where X_s is the stator reactance in Ω , X_r is the rotor reactance in Ω , X_m is the mutual reactance in Ω , I_{ds} is the stator current at d axis in A, I_{qs} is the stator current at q axis in A, I_{dr} is the rotor current at d axis in A, and I_{qr} is the rotor current at q axis in A.

The stator and rotor voltage equations are given by Eqs. (15)–(18). During start-up, the rotor in an induction generator does not require a supply of voltage. Hence the rotor voltage V_{dr} and V_{qr} are equal to zero [3]:

$$V_{ds} = -R_s \cdot I_{ds} + \omega_s \cdot \varphi_{qs} - \frac{d\varphi_{ds}}{dt} \quad (15)$$

$$V_{qs} = -R_s \cdot I_{qs} - \omega_s \cdot \varphi_{ds} - \frac{d\varphi_{qs}}{dt} \quad (16)$$

$$0 = -R_r \cdot I_{dr} + s \cdot \omega_s \cdot \varphi_{qr} - \frac{d\varphi_{dr}}{dt} \quad (17)$$

$$0 = -R_r \cdot I_{qr} - s \cdot \omega_s \cdot \varphi_{dr} - \frac{d\varphi_{qr}}{dt} \quad (18)$$

where R_s is the stator resistance in Ω , R_r is the rotor resistance in Ω , I_{ds} is the stator current at d axis in A, I_{qs} is the stator current at q axis in A, I_{dr} is the rotor current at d axis in A, I_{qr} is the rotor current at q axis in A, φ_{ds} is the stator magnetic flux at d axis in weber, φ_{qs} is the stator magnetic flux at q axis in weber, φ_{dr} is the

rotor magnetic flux at d axis in weber, φ_{qr} is the rotor magnetic flux at q axis in weber, ω_s is the synchronous speed in rad/s, and s is the slip.

The rotor slip can be calculated as follows:

$$s = \frac{\omega_s - \omega_g}{\omega_s} \quad (19)$$

where ω_s is the synchronous speed in rad/s and ω_r is the rotor speed in rad/s.

The electrical torque developed by the generator is given as follows:

$$T_e = \varphi_{qr} \cdot I_{dr} - \varphi_{dr} \cdot I_{qr} \quad (20)$$

where φ_{qr} is the rotor magnetic flux at q axis in weber, I_{dr} is the rotor current at d axis in A, φ_{dr} is the rotor magnetic flux at d axis in weber, and I_{qr} is the rotor current at q axis in A.

The power equations for the generator can then be expressed by Eqs. (21)–(23). The true power can be computed as shown:

$$P = V_{ds} \cdot I_{ds} + V_{qs} \cdot I_{qs} \quad (21)$$

The reactive power is calculated as follows:

$$Q = V_{qs} \cdot I_{ds} - V_{ds} \cdot I_{qs} \quad (22)$$

The apparent power can be written:

$$S = V_{ds} \cdot I_{ds} + V_{qs} \cdot I_{qs} + V_{qs} \cdot I_{ds} - V_{ds} \cdot I_{qs} \quad (23)$$

where V_{ds} is the stator voltage at d axis in V, V_{qs} is the stator voltage at q axis in V, I_{ds} is the stator current at d axis in A, and I_{qs} is the stator voltage at q axis in V.

2.1.4 Jensen wake model

The Jensen wake model was used to calculate the wind speed after subjecting to wake loss. The model is simplified for a single wake where the diameter of the wake is assumed to be expanding linearly. For a single wake model, the resulting wake of a wind turbine is treated to be turbulent where the near field behind the turbine is neglected. The spread of the resulting wake can be represented by the linear dimension (radius r) which is proportional to the downwind distance, x as shown in **Figure 3**. The start of the wake, u , that is directly behind the turbine is assumed to be equal to the turbine diameter:

A balance of momentum gives the following equation:

$$\pi r_0^2 u + \pi(r^2 - r_0^2)v_0 = \pi r^2 v_1 \quad (24)$$

where r_0 is the rotor blade length in m, u is the wake speed in m/s, r is the radius of wake cone in m, v_0 is the incoming wind speed in m/s, and v_1 is the resultant wake speed in m/s.

The radius of the wake cone r that represents the path of incoming wind after passing through the turbine is shown:

$$r = r_0 + \alpha x \quad (25)$$

where r_0 is the rotor blade length in m, α is the dimensionless scalar, and x is the distance from a wind turbine in m.

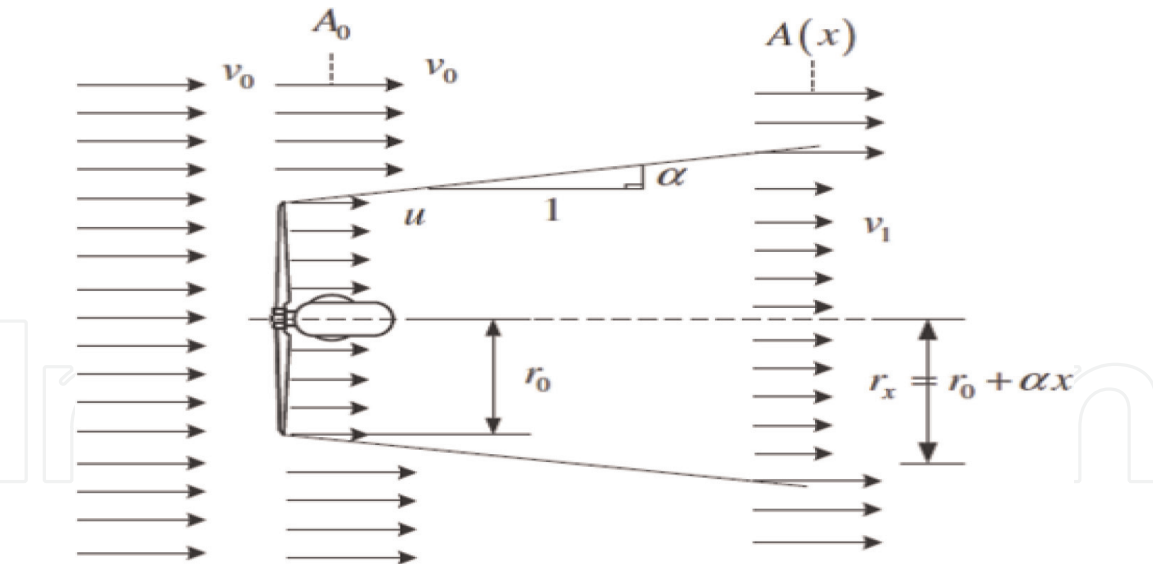


Figure 3.
 Linear expansion of wake cone for a single wake model.

The speed of wake expanding with distance which depends on the dimensionless scalar α is defined as follows:

$$\alpha = \frac{1}{2\ln\left(\frac{z}{z_0}\right)} \tag{26}$$

where z is the hub height in m and z_0 is the surface roughness.

The surface roughness constant is dependent on the characteristics of the local terrain, while the dimensionless scalar α depends on both the local terrain and wind climate conditions. The paper [2] had mentioned that a value of 0.04 can be used for α for free stream wind which has yet to pass through any wind turbine or otherwise the value of 0.08 can be assumed.

By solving Eq. (25) in terms of v_1 , the velocity of the wake at a downwind distance x from the wind turbine can be calculated:

$$v_1 = v_0 + v_0 \left(\sqrt{1 - C_T} - 1 \right) \left(\frac{r_0}{r} \right)^2 \tag{27}$$

where v_1 is the wake speed in m/s, v_0 is the incoming wind speed in m/s, C_T is the thrust coefficient, r_0 is the rotor blade length in m, and r is the radius of wake cone in m.

A thrust coefficient is a dimensionless number that defines the thrust of a wind turbine. The value of thrust coefficient varies with wind speed, and the paper [11] has shown that it has a maximum value of 1.

3. Simulation model of NordseeOst wind farm

NordseeOst is a 295 MW offshore wind farm located 35 km northeast of Heligoland, a German archipelago in the North Sea region. The wind farm consists of 48 turbines [12]. The site has an average wind speed of 9.77 m/s and an area of approximately 36 km². The site coordinates are 54° 26' 24" N and 7° 40' 48" E that are used to determine the wind condition. The layout of the wind farm used in the simulation is shown in **Figure 4**.

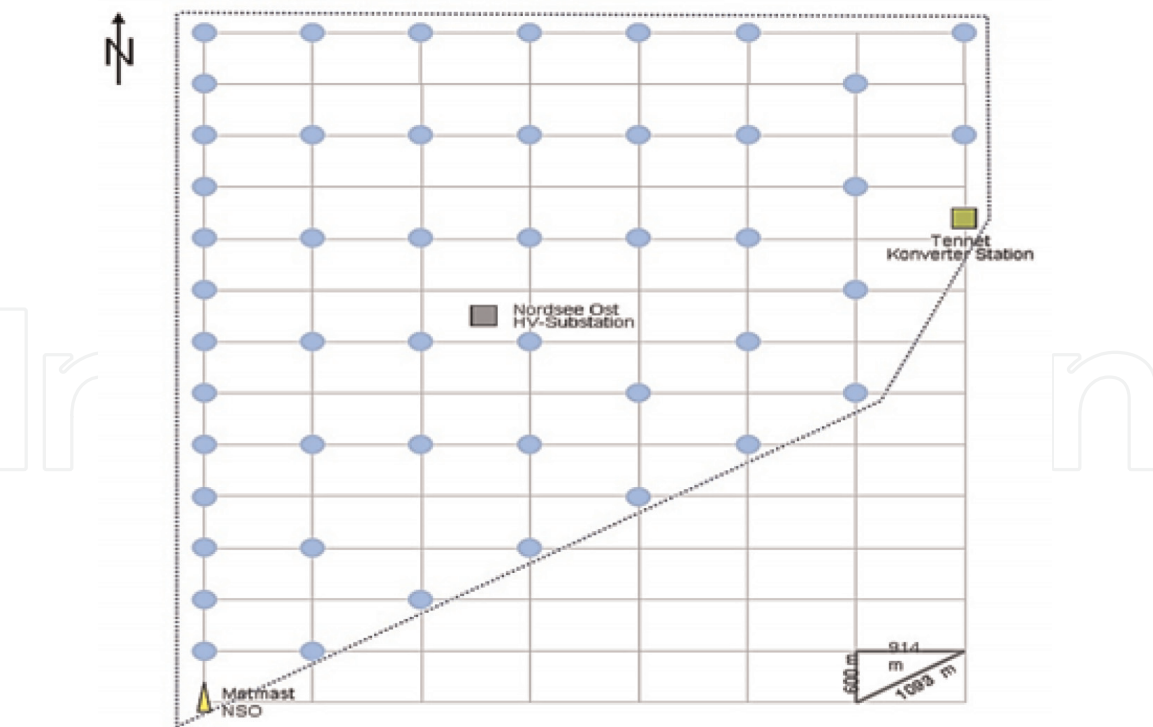


Figure 4.
Wind turbine layout of NordseeOst (RWE international SE, 2016).

The wind turbines used in the German wind farm was manufactured by Senvion. The 6.2M126 wind turbine model has a rated power of 6.15 MW and a designed rotor diameter of 126 m. The parameters for the wind turbine model presented are based on the design data provided by the manufacturer in **Tables 1** and **2**. The data from **Table 1** are the specifications for the wind turbine used in the aerodynamic and mechanical blocks. The data in **Table 2** are the parameters of the electrical system used in the induction generator block.

With all the structure and framework laid out, the next step is to implement the model in the Simulink environment. The mathematical model for each block was created and coupled together to form a wind turbine as shown in **Figure 5**. Within each respective block, few mathematical equations governing their functions as

| | |
|------------------------------|--------|
| Nominal power (kW) | 6150 |
| Cut-in wind speed (m/s) | 3.5 |
| Nominal wind speed (m/s) | 14 |
| Cutout wind speed (m/s) | 25 |
| Tip speed (m/s) | 79.8 |
| Rotor diameter (m) | 126 |
| Rotor area (m ²) | 12,469 |
| Rated rotor speed (rpm) | 12.1 |
| Hub height (m) | 92 |
| Blade length (m) | 61.5 |
| Gear ratio | 1:97 |

Table 1.
Design data for the 6.2M126 [13].

| | |
|------------------------|----------|
| Nominal power (kW) | 6150 |
| Nominal voltage (kV) | 20/30/33 |
| Nominal frequency (Hz) | 50 |
| Stator voltage (kV) | 6.6 |
| Nominal speed (rpm) | 1170 |
| Speed range (rpm) | 750–1170 |

Table 2.
Parameters for the generator [13].

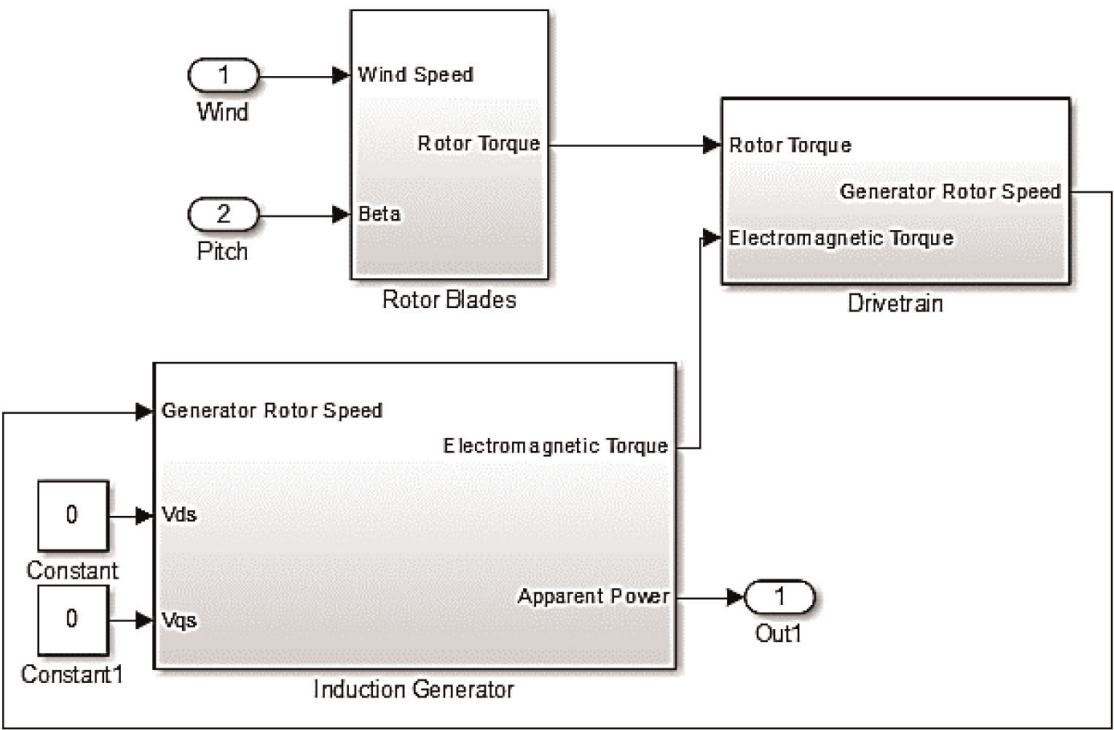


Figure 5.
Wind turbine model in Simulink.

described in Section 2.1 were modeled. The parameters available from both **Tables 1** and **2** were used in the equations.

The same approach was applied to the Jensen wake model. In the Simulink environment, the wind turbine model in blue and the wake model in red were duplicated and arranged to mimic the NordseeOst in **Figure 6**. The wake model was used when there is a wind turbine directly ahead of another. There is a spacing of one or two grid lines that corresponds to 914 m and 1828 m, respectively, with reference to **Figure 4**. For instance, the first column of wind turbines is not affected by any wake losses; hence the wake model is not required. The wind speed for the second column of turbines that are influenced by the wake effect from the first column is calculated from the first wake model block in **Figure 6**. The process is repeated for the remaining wind turbines. With a user-defined wind input, the simulation will compute the output of each turbine and collectively will be summed up to give the total power production of the wind farm.

The wind data is gathered from an online resource known as Earth. It is a visualization of global weather and ocean conditions forecasted by supercomputers. The platform is a hub of information from collective national agencies. The weather

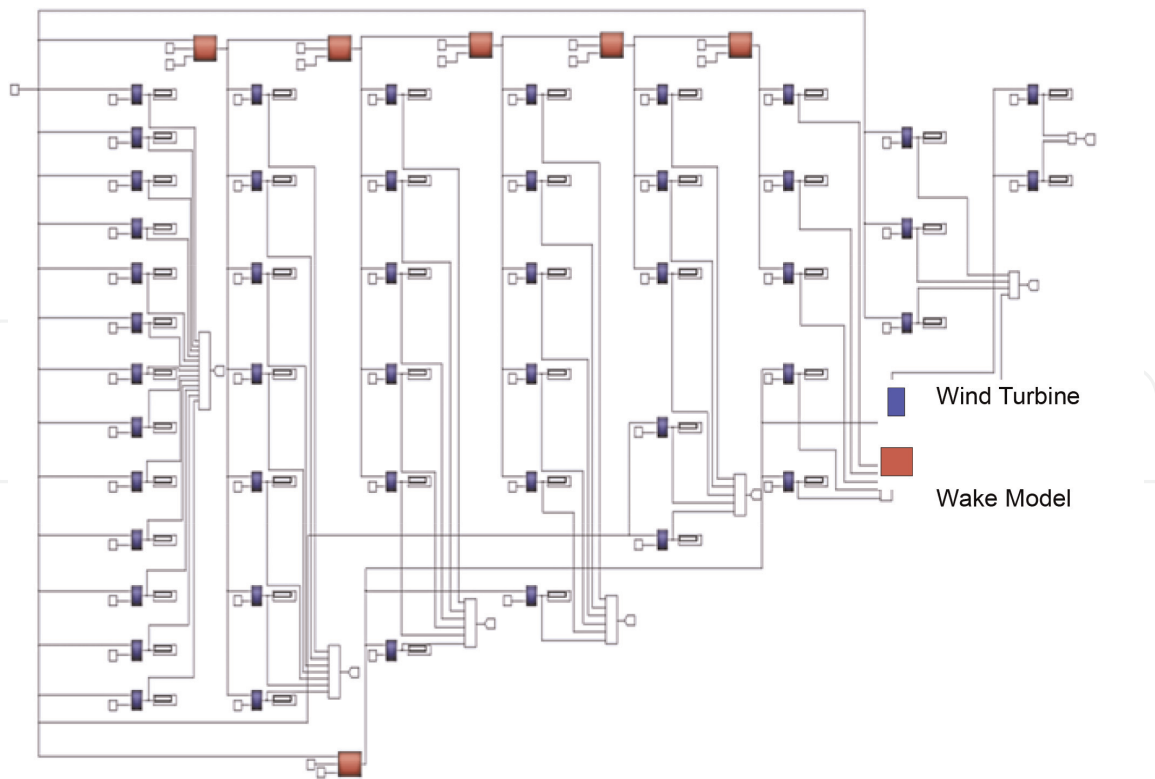


Figure 6.
Simulated NordseeOst in Simulink.

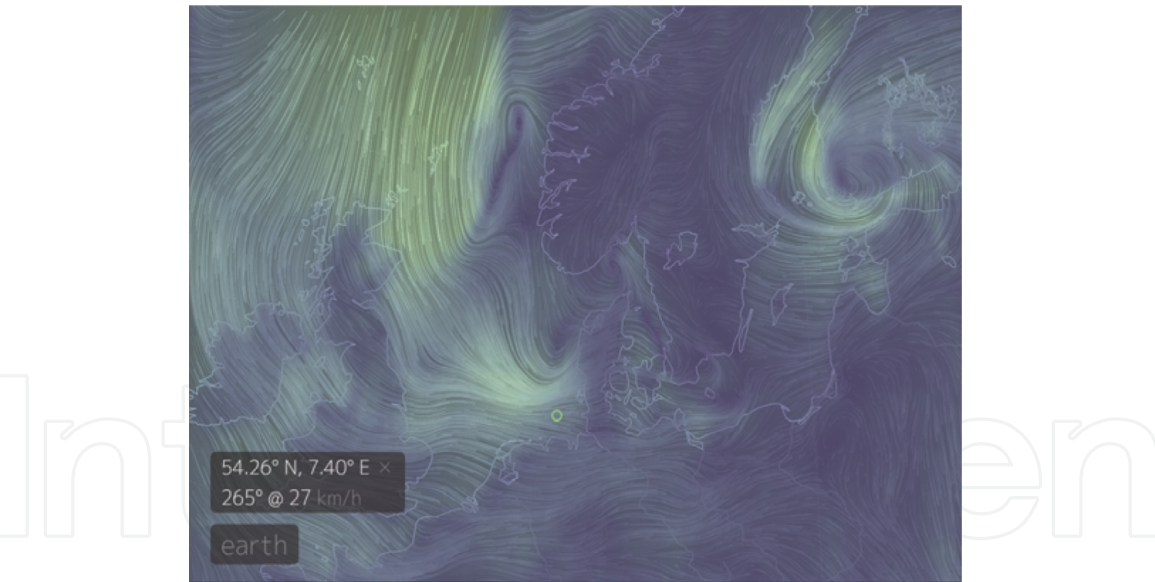


Figure 7.
Wind speed at NordseeOst from earth online.

and the wind information were obtained from the National Weather Service in the United States of America. Using the platform, the wind speed for the simulation input at any time frame was gathered from the NordseeOst coordinates as shown in **Figure 7**.

The live production data of NordseeOst in **Figure 8** is available online through an interactive map by RWE Innogy, the owner of the mentioned wind farm. This value is used as cross-reference in conjunction with the simulated results. The accuracy and functionality of the simulation can be validated by comparing the results.

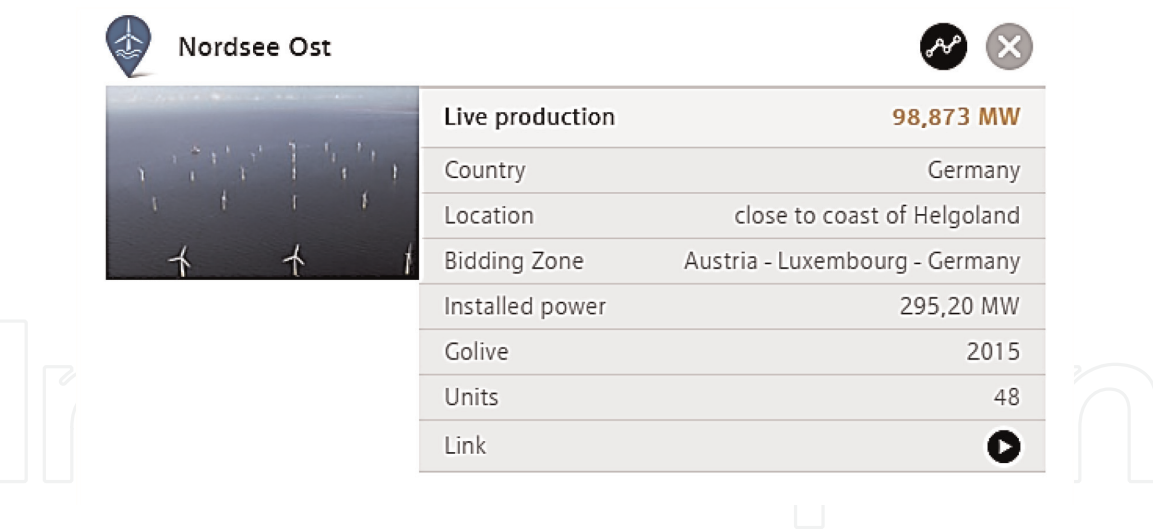


Figure 8.
Real-time output of NordseeOst [14].

4. Results and discussion

A simulation is performed over a range of wind speed 3–25 m/s at an interval of 1 m/s. The range is determined by the specified cut-in and cutout wind speed of Senvion 6.2M126 offshore wind turbine. The projected power output for the simulated farm can be seen in Figure 9. It indicates an upward trend over the increase of wind speed. From a logical standpoint, the higher the wind speed, the higher the power is generated. In the simulation, it shows the power increases with the speed of the wind. The graph shows a steady rise from the specified cut-in speed of 3 m/s where the turbine can produce useful work. It is evident that the gain begins to stabilize and reach the specified cutout speed of 25 m/s. The peak power of 300 MW is quite close to the capacity of NordseeOst at 295 MW.

Theoretically, the 295 MW should be attained at the nominal wind speed of 14 m/s according to the Senvion 6.2M126 offshore wind turbine data sheet. However, the graph included the wake losses. With the required additional wind speed

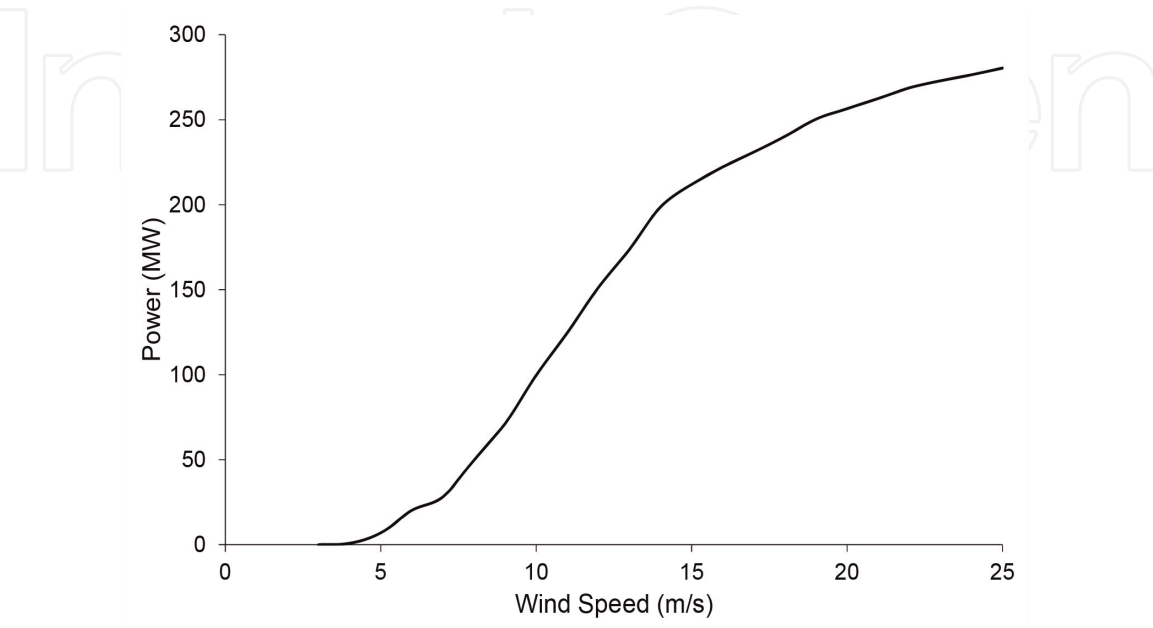


Figure 9.
Projected power output of simulated wind farm.

| Time (24 hours) | Wind speed (m/s) | Simulated (kW) | Actual (kW) | Difference (%) |
|-----------------|------------------|----------------|-------------|----------------|
| 0800 | 5.1 | 8099 | 7816 | 3.49 |
| 1100 | 7.4 | 35,958 | 33,339 | 7.86 |
| 1400 | 10.5 | 112,555 | 110,678 | 1.70 |
| 1700 | 10.0 | 99,691 | 95,611 | 4.27 |
| 2000 | 6.4 | 23,686 | 22,434 | 5.58 |
| 2300 | 6.6 | 25,104 | 23,297 | 7.76 |
| | | | Average | 5.11 |

Table 3.
Three hourly data log.

of 11 m/s to achieve a rated output, it is evident that wake losses play a significant role in power efficiency. It emphasizes the importance of optimizing the wind turbine position to reduce the effect of wake losses. From the results gathered in the study of NordseeOst, it can be observed that the wind farm layout optimization can be further improved.

As seen in **Table 3**, a test run was performed with a wind speed of 5.10 m/s in a particular period. The resulted power output of the simulation is 8099 kW, while the actual power from the wind farm is 7816 kW. There exists a difference of 3.5% in the results. Due to the limitation of the Earth where the weather forecast was updated every 3 hours, reading was taken every 3 hours for 18 hours to check for consistency. The average difference of 5.11% can be seen in **Table 3**. There are several possible reasons for the discrepancy. One possible reason could be due to the sizing of components in the mechanical and electrical systems. With the absence of a physical system, the parameter of inertia, damping and stiffness coefficient in the drivetrain, and components such as resistance, inductance, and reactance in the induction generator are not readily available.

Another possible reason is the lapse in representing wake losses in a wake model. The Jensen wake model provides a simple and reasonably accurate representation. The orientation of turbine layout and wind direction will affect the direction and position of the wake cone. As a result, it caused the interaction of wake cones and altered the effect on wake loss. It is indicative that the Jensen wake model may have underestimated the effect of wake loss. Hence, further studies in improving the Jensen wake model are needed.

Another reason is the limitations of the wind forecast that is updated only every 3 hours. It is not synchronized with the live production data from RWE. It could cause some slight deviation in the simulated results. The availability of the actual wind speed at the wind farm site will be useful. It will allow a better and more accurate model validation.

However, the results attained are valid and have the potential for simulating and analyzing a wind farm. This methodology offers a solution in modeling the wind farm before any site implementation. It can contribute to future wind energy-related studies that have not been addressed in the literature of wind farm modeling and simulation for smart cities.

5. Conclusions

The systematic approach in simulating an offshore wind farm model was presented. The simulation tool was used to predict the output power projection with

consideration of the wake loss using Jensen wake model. The wind turbine model was adapted from Senvion 6.2M126 offshore wind turbine. Based on the case study of NordseeOst wind farm in Germany, the wind farm was replicated with multiple completed wind turbines with consideration of the wake model. The application of the wind farm was validated with wind speed ranging from 3 to 25 m/s. The simulated results were compared with the real-time data from the NordseeOst wind farm. The average difference is approximately 5.11%. The same approach can be used in the design and developmental phase of any wind farm to predict the output power for smart cities.

For future works, the wind turbine model can be enhanced by incorporating details and intricate representative of various systems used in the modeling. The simulation results can be verified by comparing with other simulation tools such as Wind Atlas Analysis and Application Program (WAsP). An improved wake loss model and layout optimization will be considered in future studies.

Acknowledgements

The author would like to express his sincere gratitude to the staff of Newcastle University in the United Kingdom for their continuous support and encouragement.

Conflict of interest

There is no conflict of interest in this chapter.

Author details


Cheng Siong Chin^{1*}, Chu Ming Peh¹ and Mohan Venkateshkumar²

1 Faculty of Science, Agriculture, and Engineering, Newcastle University in Singapore, Singapore

2 Department of Electrical and Electronics Engineering, The Aarupadai Veedu Institute of Technology, Chennai, India

*Address all correspondence to: cheng.chin@ncl.ac.uk

IntechOpen

© 2020 The Author(s). Licensee IntechOpen. Distributed under the terms of the Creative Commons Attribution - NonCommercial 4.0 License (<https://creativecommons.org/licenses/by-nc/4.0/>), which permits use, distribution and reproduction for non-commercial purposes, provided the original is properly cited. 

References

- [1] Sun X, Huang D, Wu G. The current state of offshore wind energy technology development. *Energy*. 2012; **41**(1):298-312
- [2] González-Longatt F, Wall P, Terzija V. Wake effect in wind farm performance: Steady-state and dynamic behavior. *Renewable Energy*. 2012; **39**(1):329-338
- [3] Martinez J. Modelling and control of wind turbines [Master thesis]. UK: Imperial College London; 2007
- [4] Singh M, Santoso S. Dynamic Models for Wind Turbines and Wind Power Plants. Texas: National Renewable Energy Laboratory; 2011
- [5] Bekker J. Efficient modelling of a wind turbine system for parameter estimation applications [Master thesis]. South Africa: Stellenbosch University; 2012
- [6] Ahmadi M. Analysis and study of floating offshore wind turbines [Master thesis]. US: University of Toledo; 2013
- [7] Saheb-Koussa D, Haddadi M, Belhamel M, Koussa M, Nouredine S. Modeling and simulation of Windgenerator with fixed speed wind turbine under Matlab-Simulink. *Energy Procedia*. 2012;**18**:701-708
- [8] Gagnon R. 2016. Wind Farm (IG)—MATLAB & Simulink Example. Mathworks.com. Available at: <http://www.mathworks.com/help/physmod/sps/examples/wind-farm-ig.html> [Accessed: 02 January 2018]
- [9] Betz A. Wind-Energie und ihre Ausnutzung durch Windmühlen. Göttingen: Vandenhoeck; 1926
- [10] Chong N, Ran L. Offshore Wind Farms: Technologies, Design and Operation. United Kingdom: Woodhead Publishing; 2016. <https://www.amazon.com/Offshore-Wind-Farms-Technologies-Publishing/dp/0081007795>
- [11] Manwell J, McGowan J, Rogers A. Wind Energy Explained. Chichester, UK: Wiley; 2009
- [12] RWE. 2016. Nordsee Ost. Available at: <http://www.rwe.com/web/cms/en/400596/rwe-innogy/sites/wind-offshore/in-operation/nordsee-ost/> [Accessed: 02 January 2018]
- [13] Wind Turbine Model 6.2M126. 2016. Available at: <https://www.senvion.com/global/en/wind-energy-solutions/wind-turbines/6xm/62m126/> [Accessed: 02 January 2018]
- [14] RWE Innogy. 2016. Rwe-renewableslive.com. Available at: <http://rwe-renewableslive.com/#/map/EU/NSO1> [Accessed: 02 January 2018]